Centrifugal casting of complex geometries: Computational modelling and validation experiments

Shevchenko, D. M.; McBride, D.; Humphreys, N. J.; Croft, T. N.; Withey, Paul; Green, N. R.; Cross, M.

CENTRIFUGAL CASTING OF COMPLEX GEOMETRIES: COMPUTATIONAL MODELLING AND VALIDATION EXPERIMENTS

D. M. Shevchenko[1], D. McBride[2], N. J. Humphreys[1], T. N. Croft[2], P. Withey[3], N. R. Green[1], M. Cross[2]

[1]The University of Birmingham, Edgbaston, Birmingham, B15 2TT. UK
[2]Swansea University, Singleton Park, Swansea, SA2 8PP. UK
[3]Rolls-Royce Plc, P.O. Box 31, Derby, DE24 8BJ. UK

Keywords: computational modelling, centrifugal casting, free surface modelling, gas entrainment

Abstract

Centrifugal casting offers one route through to high quality products in difficult to cast high temperature low superheat alloys. The coupling of free surface flows and complex rotating geometries, resulting in significant centrifugal forces, combined with rapid heat transfer and solidification yields a significant computational modelling challenge. The objective of the work reported here is to develop a comprehensive computational model of centrifugal casting that can reliably predict the macro-defects that arise from the process. In this contribution we describe:

- A computational framework for modelling the filling and solidification of centrifugal castings,
- a series of large scale centrifugal casting experiments with the full complexity of a target industrial system, together with
- a sensitivity study of a principal boundary conditions.

Introduction

Two of the principal drivers of the development of modern aircraft engines are the requirement for increased engine efficiency and reduced environmental impact. In part, this can be achieved by using new materials and new design of turbine blades. Materials which offer an attractive balance of properties and may show a path to achieving these goals often have to be formed into geometries which are difficult to manufacture. New materials in this field [1] tend to be highly reactive with the processing environment leading to other processing issues such as low superheat due to the use of induction skull melting. Components such as low pressure turbine blades which can best utilise the properties on offer tend to be characterised by thin aerofoil sections of a few millimetres thickness and hundreds of millimetres length. This results in limited filling of thin section components if casting using conventional gravity methods [2].

Centrifugal casting is an attractive method for the production of thin section castings as, under the action of the centrifugal force, metal can overcome the backpressure due to surface tension and fill mould sections with thicknesses substantially less than a millimetre. However, due to the low superheat and high liquid metal velocity developed there is a high risk of free surface turbulent flow and of the associated entrainment through free surface turbulence [3] and trapping of gas present in the flow [2]. It is therefore essential that casting process simulation tools are able to represent these effects.

A numbers of process simulation tools have been applied to simulate liquid metal flow during centrifugal casting [4]-[11]. All reported that the filling process played an important role in determining casting quality. Shiping *et al.* [4] and Changyun [9] used water experiments to validate their model and showed that back pressure effects must be accounted for. Examples of commercial software packages that have been applied to successfully simulate centrifugal casting include MAGMASOFT and ProCAST. Using ProCAST Fu *et al*. [10] showed the possibility of the prediction of the solidification shrinkage formation during centrifugal casting of TiAl alloy car valves. Sung *et al*. [11] used MAGMASOFT to simulate centrifugal casting of TiAl alloy turbocharger castings and found that the simulation result strongly depended on the boundary conditions applied and physical properties of alloy. However, despite the successes reported above, in order to resolve fully within a model bubble formation, transport, rejection from the liquid or capture by the solidifying front it is necessary to develop a two phase (liquid+gas) model.

The aim of the work reported in this paper is to validate numerical techniques that can adequately capture the physics to predict behaviour in the centrifugal casting of large thin wall structural engineering components. Capturing the liquid-gas interface, gas entrainment and transport of bubbles on these complex geometries, coupled with centrifugal forces, heat transfer and solidification make this a significant computational modelling challenge. A model has been developed within the computational framework of PHYSICA [12], where numerical procedures are based on a finite volume formulation for unstructured three-dimensional heterogeneous meshes. The model was initially validated against a number of high quality water experiments in the prediction of the initial fluid film, vortex formation and trend in air bubble creation and transport within the system. The work found that accurate representation of the inlet pour conditions was vital to the generation of bubbles and their transport within the mould. Experimental observations showed that the metal pour does not necessarily enter the system as a constant stream. Inevitably, in an unconstrained pour, there is some spatial movement and slight variations in the flow rate. The flow dynamics are difficult to capture and a series of aluminium alloy castings have been produced in order to calibrate and validate the model.

Computational Model

The model has been implemented within, PHYSICA [12], a finite volume simulation tool employing unstructured heterogeneous meshes for complex 3D geometries and with scalable speed-up in parallel [14].

Governing equations

The liquid metal and the air are represented as a Newtonian fluid by the Navier-Stokes equations:

a) for fluid momentum

$$\frac{\partial(\rho \underline{u})}{\partial t} + \nabla.(\rho \underline{u}\,\underline{u}) = \nabla.\left(\mu_{eff} \nabla \underline{u}\right) + \underline{S}_u - \nabla p \tag{1}$$

b) for mass conservation

$$\frac{\partial \rho}{\partial t} + \nabla.\left(\rho \underline{u}\right) = S_m \tag{2}$$

where $\underline{u}$ is the fluid mixture velocity, ρ is the fluid mixture density, p is pressure and μ_{eff} is the effective viscosity.

The governing equations are solved in a non-inertial reference frame, where the co-ordinate system moves with the rotating equipment. To account for the acceleration of the fluid the centrifugal and coriolis forces enter the momentum equations as fictitious forces. The velocity of the fluid relative to the co-ordinate system can be expressed as;

$$\underline{u}_r = \underline{u} - (\underline{\Omega} x \underline{r}) \tag{3}$$

Substituting (3) into (1) and re-arranging the left hand side of (1) can be written as;

$$\frac{\partial}{\partial t}\left(\rho \underline{u}_r\right) + \nabla.\left(\rho \underline{u}_r \underline{u}_r\right) + \rho\left(2\underline{\Omega} x \underline{u}_r + \underline{\Omega} x (\underline{\Omega} x \underline{r})\right) \tag{4}$$

and equation (2) as;

$$\frac{\partial \rho}{\partial t} + \nabla.\left(\rho \underline{u}_r\right) = S_m \tag{5}$$

When the fluid is rotating at the same velocity as the rotating frame the forces should balance and the relative velocity is equal to zero. The differencing scheme employed in the numerical discretisation of the governing equations is crucial to ensuring the balance of forces and hence the correct time period for a stationary fluid to achieve its rotational velocity. A first order scheme is not sufficient and a higher order scheme such as, SMART is required.

The free surface flow uses a fixed grid approach and employs the FV-UM scheme of Pericleous [14], which solves the advection of a scalar,

$$\frac{\partial \phi}{\partial t} + \nabla \cdot (\phi \underline{u}_r) = S_\phi \tag{6}$$

The method captures the interface as a discontinuity in the solution field, the GALA scheme developed by Spalding [13] combined with a Donor Acceptor [15] to ensure the interface remains sharp as it convects through a fixed mesh.

The heat transfer and solidification are described by:

$$\frac{\partial}{\partial t}(\rho\, c T) + \nabla.(\rho \; c \; \underline{u} \; T) = \nabla.(k \nabla T) + S_h \tag{7}$$

where c is the mixture specific heat capacitance and k the conductivity. The source term S_h can represent viscous dissipation, heat due to fluid bulk motion, boundary heat transfer and the latent heat release during phase change. If only change of phase is considered, the source into the heat equation due to the solidification process is equal to:

$$\boldsymbol{S_h} = -\frac{\partial(\boldsymbol{f_L L})}{\partial \boldsymbol{t}} - \nabla.(\boldsymbol{\rho \underline{u} f_L L}) \tag{8}$$

where L is the latent heat of solidification and f_L is the liquid fraction of the metal component of the fluid. The liquid fraction is typically a function of the metal temperature, where the liquidus temperature is the temperature at which the metal is fully liquid and the solidus temperature is the temperature at which the metal has totally solidified;

Experimental Procedure

Two types of casting were made validate the computational model simulations: a gravity casting into a sand mould with the filling recorded using real-time x-ray imaging of the liquid metal flow and secondly investment moulds were centrifugally cast at low superheat from an induction skull melting (ISM) furnace.

Gravity (stationary) casting

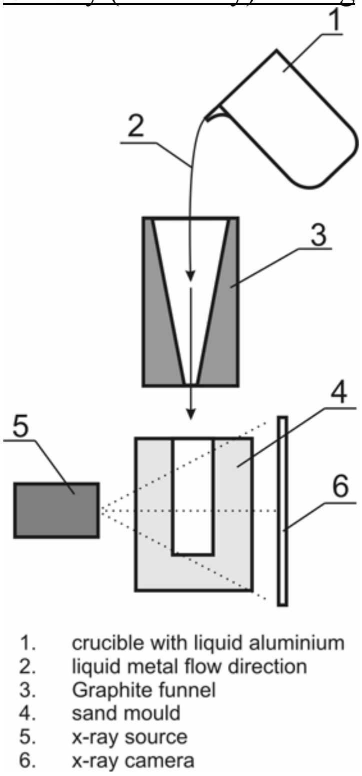

Figure 1: Experimental setup of the gravity casting with x-ray metal flow recording

The gravity casting was done to establish the structure the pouring metal stream and generate data with which to validate the model. The setup of the experiment is shown in Figure 1. An aluminium alloy (6082) with the temperature of 700 ºC was poured from a crucible (1) to the sand mould (4) through a graphite funnel (3). The sand mould had the following dimensions: 200mm high, 100 mm width and 50 mm depth. The experiment setups such as pouring height, crucible tilt rate, metal superheat and metal superheat were selected to reproduce the conditions when centrifugally casting from the ISM furnace. The flow was recorded at a resolution of 800×600 pixels at frame capture rate of 60 s^{-1} and a field of view equating to a nominal resolution of 3.5 pixels/mm.

Centrifugal casting in ISM furnace

Two mould designs (see Figure 2) with indirect gating systems were selected for the centrifugal casting experiment. Before casting moulds were preheated remotely such that at the time of casting the mould temperature was 400 ±10 ºC. The pouring metal temperature was 700 ±5 ºC. During casting the box with investment casting mould was rotating with a rotation speed of 400 rpm. The duration of rotation was 3 minutes.

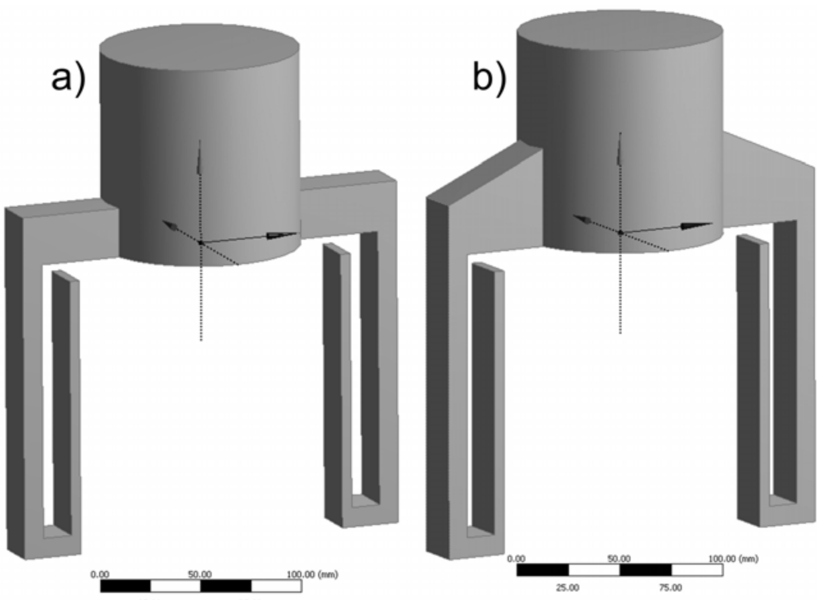

Figure 2: Mould designs for centrifugal casting experiments; a) Mould 1, b) Mould 2

Numerical Model

The meshes comprised of a combination of hexahedral and pentahedral elements. Mould 1 having 234,360 elements and Mould 2 having 335,040 elements. An outlet boundary condition of zero pressure was applied to the tip of the inverted gate. A zero pressure boundary was also set at the outer top surface of the cylinder. A variable inlet condition was applied at the centre of the top surface. The metal was transferred into the cylinder at an average rate of 1.5kg/s over 2seconds. The central inlet assumed an average pour diameter of 25mm with fluctuations in the inlet diameter expressed by;

$$diameter_{inlet} = 25 + (\pi + 1.5\theta)\sin(300t) \tag{9}$$

where θ is the inlet angle and t is the simulation time.

Results and Discussion

Gravity (stationary) casting

Figure 3 shows still frames extracted from the real-time x-ray filling sequence. It can be observed that during filling the metal stream generated a large number of bubbles with resolved sizes ranging between 3 mm and 30 mm in diameter. In the early stages of pouring the brightness of the image reflects the very low bulk density of the fluid. Similarly, at the end of metal pouring (Fig. 3(d)) the fluid contains an emulsion of bubbles that in Figure 3(e) have resulted in formation of an unstable metal froth on the surface. It can also be seen in Figure 3 that the incoming liquid stream is itself unstable and, as the pouring profile and geometry configuration matches that of the ISM the perturbation of the inlet condition will also occur during casting from the ISM furnace.

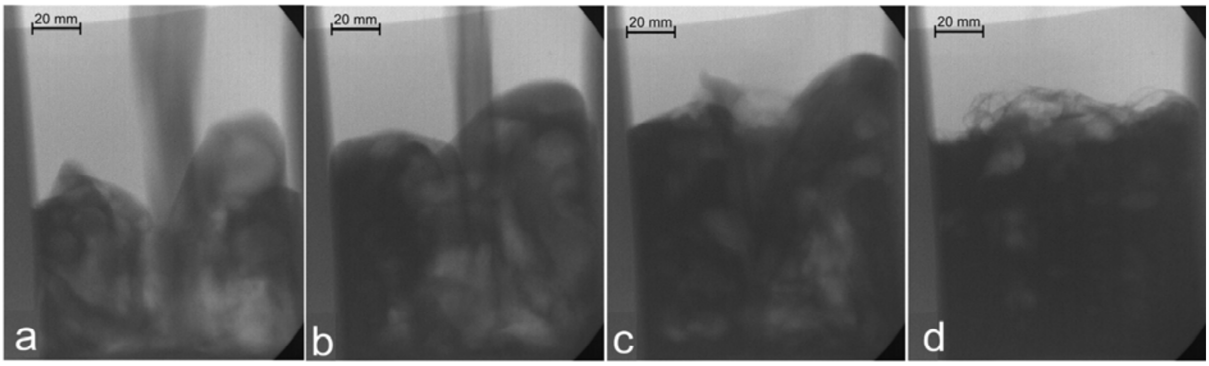

Figure 3. X-ray of the mould filling during gravity casting at different time from the start of pouring; a) 0.5s; b) 0.68s; d)0.91s; e) 1.15s

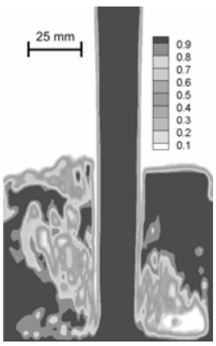

Figure 4. Cross section plot of liquid metal volume fraction, perturbed inlet condition, 0.65 s

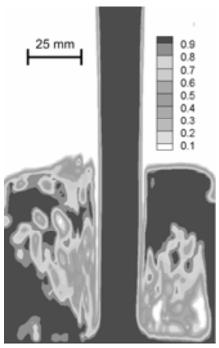

Figure 5. Cross section plot of liquid metal volume fraction, constant inlet condition, 0.65 s

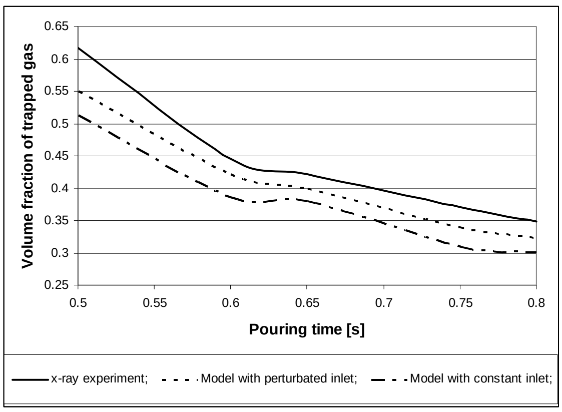

Figure 6. Volume fraction of trapped gas in liquid/bubble mixture

Key images of the simulated filling are shown in Figure 4 and 5. It can be seen that the liquid contains a high fraction of gas, occupying a volume significantly greater than the theoretical value. A distribution of bubble sizes are resolved and the transport to and escape from the liquid surface is observed. It is also observed that, as in the metal casting experiments and previous water modelling studies [17], large bubbles are fragmented into dispersions of smaller cavities. Figure 6 compares the measured and calculated volume of gas within the liquid/bubble mixture. Data from the initial transient, in which the liquid flows up the side walls of the mould has been discarded. It is found that the actual gas volume is consistently less than the calculated volume. However, significant error in measurements from the experimental data may arise due to the 2D nature of the data. Introduction of a variable inlet condition, determined previously as necessary to reflect correctly the form of the incoming liquid stream can be seen to have increased the fraction of gas in the liquid.

Centrifugal casting

Figures 7 and 9 show details of macro defects within the castings. Both castings contain large pockets of gas that have also acted as nucleation sites for additional shrinkage porosity (labelled A to E). Multiple castings showed almost identical sizes and locations of defects. Results of the simulated filling of castings equivalent to Figures 7 and 9 are shown in Figures 8 and 10. It is evident that in both instances the modelled results correlate closely with the experimental data. Extensive bubble creation is observed within the central core into which the metal was poured and individual bubbles can be resolved moving within the liquid, becoming concentrated, under the action of the centrifugal pressure gradient, at the inward surfaces. Similarly larger gas pockets are found to be concentrated at regions of low pressure within the liquid.

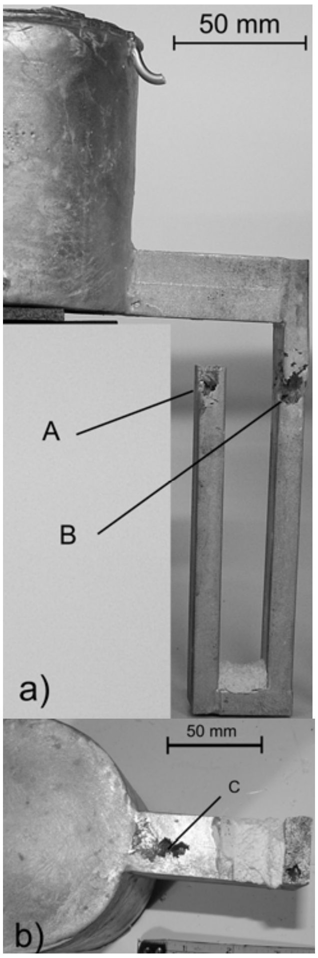

Figure 7.Side (a) and bottom(b) views of casting1

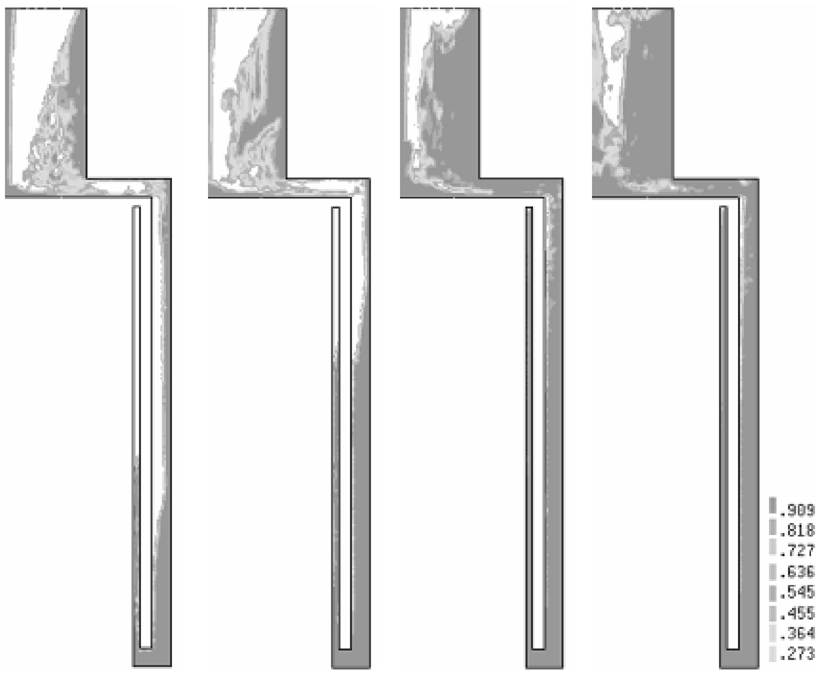

a (0.44 s) b (0.66 s) c (1.32 s) d (1.54 s)

Figure 8. Volume fraction of liquid Al alloy. Cut plane through the centre line of the horizontal runner

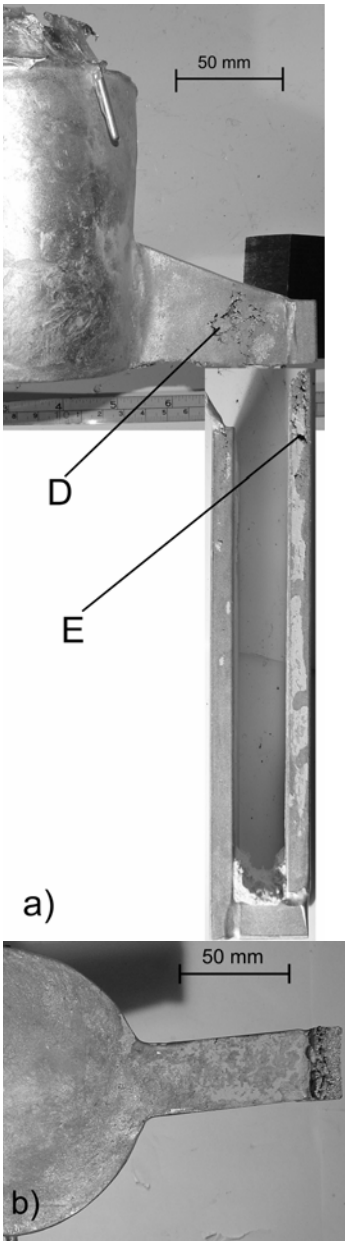

Figure 9. Side (a) and bottom (b) views of casting2

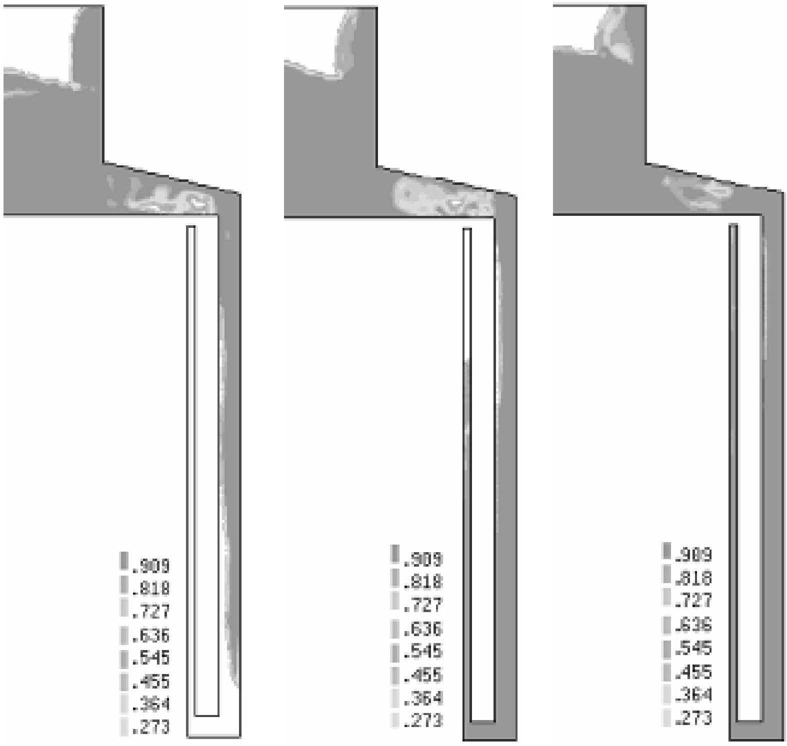

a (0.22 s) b (0.66 s) c (1.32 s)

Figure 10. Surface fluid fraction plotted at different phases of casting filling.

When the design of the runner connecting the central pouring core to the outer downward sprues was modified to increase the inlet cross sectional area (Figures 9) it was found that the volume of gas within the defects D and E was reduced relative to those in the other casting (labeled A and B). This effect is reproduced clearly within the model. Similarly motion of small bubbles within the metal stream can be identified in Figure 8a, where they are carried within the flow around the base of the downsprue into the vertical strip casting. Thus, whilst the model accurately reflects the two phase flow it can be concluded that filling methods such as those investigated are unlikely to enable casting of bubble free components.

Conclusions

A casting process model has been developed within a finite volume unstructured simulation framework that enables detailed and accurate modelling of the two phase flow during filling of complex geometries. A series of casting experiments have been conducted to validate the model and it was found that there is close correlation of the fraction of gas incorporated into the liquid during pouring and filling. The filling and bubble entrainment was described most accurately when a perturbed inlet boundary condition was incorporated.

The model developed highlighted the importance of considering the mixing of the two phase liquid+gas system during metal pouring in centrifugal casting if defect free components are to be obtained.

Acknowledgement

One of the authors (NG) is indebted to EPSRC for their support of the Chair in Casting Technology under grant EP/D505569/1.

References

[1] Wu X., "Review of alloy and process development of TiAl alloys", *Intermetallics*, 14 (2006), 1114-1122

[2] R.A. Harding, M. Wickins, and Y.G. Li, "Progress towards the production of high quality γ-TiAl castings," Structural Intermetallics 2001. Proceedings of the Third International Symposium on Structural Intermetallics, 23-27 Sept. 2001, 181-189.

[3] Campbell J., *Castings* (Oxford, UK: Butterworth-Heinemann, 2003), 17-69

[4] W. Shiping et al., "Numerical simulation and experimental investigation of two filling methods in vertical centrifugal casting," *Transaction of Nonferrous Metals Society of China*, 16 (2006), 1035-1040.

[5] W. Shiping et al., "Numerical simulation of microstructure evolution of Ti-4Al-4V alloy in vertical centrifugal casting," *Materials Science and Engineering*, 426 (2006) 240-249

[6] W. Shiping et al., "Numerical simulation of off-centred porosity formation of TiAl-based alloy exhaust valve during vertical centrifugal casting", *Modelling and Simulation in Materials Science and Engineering*, 11 (2003), 599-608.

[7] S. Wen-bin, "Filling and solidification of TiAl melt in centrifugal field", *Transaction of Nonferrous Metals Society of China*, 16 (2006), 719-722.

[8] S.R. Chang, J.M. Kim, and C.P. Hong, "Numarical simulation of microstructure evolution of Al alloy in centrifugal casting," *ISIJ International* 41 (2001), 738-747.

[9] L. Changyun et al., "Hydraulic modelling of mould filling behaviour during vertical centrifugal casting," *International Journal of Cast Metals Research*, 19 (2006), 237-240.

[10] P.X. Fu et al., "Centrifugal casting of TiAl exhaust valves," *Intermetallics*, 16 (2008) 130-138.

[11] Si-Young Sung, Young-Jig Kim, "Modeling of titanium aluminides turbo-charger casting," *Intermetallics*, 15 (2007) 468-474

[12] PHYSICA, see http://physica.co.uk

[13] K McManus et al., Assessing the parallel performance of multi-physics tools for modelling of solidification and melting processes, *Intl Jnl High Perf Comp Applns*, 19, 1-27 (2005)

[14] K Pericleous et al. "Three Dimensional Free Surface Modelling in an Unstructured Mesh Environment for Metal Processing Applications," *Applied Math Modelling*, Vol. 22, pp.895-906, (1998)

[15] D B Spalding, "Mathematical modelling of fluid mechanics, heat transfer and chemical reaction processes," *Report HTS – 80-1*, Mech Engg Dept, Imperial College London (1980)

[16] J B Ramshaw and J A Trapp, "A numerical technique for low speed homogeneous two phase flow with a sharp interface," *Journal of Computational Physics*, 21, pp 438-453 (1976)

[17] D. McBride et al., "Complex free surface flows for mould filling using centrifugal casting," Modeling of Casting, Welding and Advanced Solidification Processes XII, June 7-14, 2009, Vancouver, Canada